The Mechanism of the Solvent Perturbation of the $a^1\Delta_g \rightarrow X^3\Sigma_g^-$ Radiative Transition of O_2

Reinhard Schmidt,* Farokh Shafii, and Markus Hild

Institut für Physikalische und Theoretische Chemie, J. W. Goethe-Universität, Marie-Curie-Strasse 11, D60439 Frankfurt am Main, Germany

Received: November 17, 1998; In Final Form: January 26, 1999

The rate constants k_{b-a} and k_{a-X} of the $b^1\Sigma_g^+ \rightarrow a^1\Delta_g$ and $a^1\Delta_g \rightarrow X^3\Sigma_g^-$ emissions of O_2 have been determined in liquid CCl_4, C_2Cl_4, and C_4Cl_6. The ratios k_{a-X}/k_{b-a} range from 4.4×10^{-4} (CCl_4) to 8×10^{-4} (C_4Cl_6). In addition, rate constants k_{a-X} have been determined in several solvents and in the binary solvent mixtures H_2O/acetone, acetone/C_6H_6, and $CH_3OH/CHCl_3$. k_{a-X} depends for H_2O/acetone and $CH_3OH/CHCl_3$ in a strongly anomalous way on the bulk polarizability P of the solvent, demonstrating that no general smooth correlation of k_{a-X} with P exists. Our results confirm the perturbation model developed by Minaev. According to this model, the collision-enhanced b → a radiative transition lends intensity to the transition a → X. Both radiative transitions are bimolecular processes. For the pure solvents, the second-order rate constants k^c_{a-X} correlate roughly with the square of the molar refraction R of the solvent. If the effects of the solvent refractive index, of the collision frequency, and of the dependence of the probability P_{a-X} of the collision-induced radiative transition per collision on the size of the collider, are removed, a direct and linear proportionality of the transition moment of the collision-induced emission with the collider's molecular polarizability is discovered. For mixtures, k_{a-X} is additively composed of the contributions of the individual components. These results explain for the first time consistently and quantitatively the solvent effects on k_{a-X}.

Introduction

Two excited singlet states, $b^1\Sigma_g^+$ and $a^1\Delta_g$, lie closely above the $X^3\Sigma_g^-$ triplet ground state of O_2.[1] Since transitions between any two of these three states are of the type g−g, they are strictly forbidden by the selection rules for electric dipole radiation. Spin−orbit interaction leads to a magnetic dipole character of the a → X phosphorescence,[2] which occurs for the isolated molecule at 1269 nm with the very small radiative rate constant $k_{a-X} = 2.6 \times 10^{-4}$ s^{-1}.[3] k_{a-X} is by several orders of magnitude larger in solution and varies from about 0.2 (H_2O) to 4 s^{-1} (CH_2I_2).[4−9] Ogilby et al.[8] compiled their own and literature data.[4,6,7,9−15] Their analysis revealed no correlations of k_{a-X} with the dielectric constant ϵ or functions of ϵ. However, rather smooth and upward curved empirical correlations of k_{a-X} with the solvent refractive index n or with functions of n, e.g., the bulk polarizability $P = (n^2 - 1)/(n^2 + 2)$ can be found.[8] It was proposed that such correlations could be used to accurately predict values of k_{a-X} for solvents not yet investigated. However, by investigations in solvent mixtures, Bilski et al. recently presented some evidence that a general smooth correlation of k_{a-X} with P apparently does not exist.[16] Speculation that the solvent dependence of k_{a-X} could be interpreted on the basis of a Kirkwood/Onsager reaction field model, considering the solvent as a homogeneous and isotropic dielectric medium,[8] could not be verified.

A different perspective of the solvent effect on k_{a-X} considers the role of bimolecular collisions of $O_2(^1\Delta_g)$ with solvent molecules.[17] The intensity enhancement of the a → X phosphorescence was related by Minaev with a corresponding collision-induced enhancement of the $b^1\Sigma_g^+ \rightarrow a^1\Delta_g$ fluorescence.[18,19] This emission is allowed only as an electric quadrupole transition for the isolated molecule and occurs in the diluted gas at 1908 nm with the very small radiative rate constant $k_{b-a} = 2.5 \times 10^{-3}$ s^{-1}.[20] Minaev showed that the b → a transition gets considerable dipole character in collisions. Because of the strong spin−orbit coupling of O_2, the X ground-state acquires some $^1\Sigma_g^+$ character. Therefore, the a → X transition should profit from the collision-induced enhancement of the b → a band by intensity borrowing, leading to the prediction of proportionality of the rate constants of the respective collision-induced radiative processes for a given collider.[18,19] We recently presented compelling evidence for the validity of Minaev's perturbation model.[17] Moreover, we demonstrated that second-order rate constants k^c_{b-a} and k^c_{a-X} of the collision-induced radiative transitions depend in a very similar way on the molecular polarizability of the collider. Both k^c_{b-a} and k^c_{a-X} have been found to be nearly proportional to the square of the molar refraction R of the collider, indicating a direct proportionality of the induced transition moments with the collider's molecular polarizability.[17] Despite these results, Minaev's perturbation model is still not generally accepted. The possibility of interpreting the anomalous dependence of the first-order rate constant k_{a-X} on the bulk polarizability P in mixtures of D_2O and acetonitrile on the basis of our findings by means of second-order rate constants k^c_{a-X} of both components was ignored.[16] Instead, it was speculated that specific interactions, i.e., complex formation between $O_2(^1\Delta_g)$ and the π bonds of the −CN moiety, could be the reason for the anomalous behavior of k_{a-X}. Therefore, we felt that further investigations would be useful to reveal the physical reason for the solvent effects on the b → a and a → X emissions of O_2.

Experimental Details

CCl_4 (Acros, 99+%), C_2Cl_4 (Merck, Uvasol 99.8%), C_4Cl_6 (Fluka, 97%), CS_2 (Fluka, 99%), CH_3OH (Riedel-de Haen,

10.1021/jp984458n CCC: $18.00
Published on Web 03/20/1999

99.8%), $CHCl_3$ (Aldrich, 99.8%), and C_6H_6 (Aldrich, 99+%) were dried by column chromatography (Al_2O_3). D_2O (MSD Isotopes, 99.9 at. %) was taken as supplied. The rest of solvents used for the investigation of $O_2(^1\Delta_g)$ were of highest purity available and used as received. The singlet oxygen sensitizer phenalenone (Aldrich, 97%) was purified by column chromatography (CH_2Cl_2/silica gel). C_{60} (Fluka, 98%+) was taken as supplied. In the investigation of $O_2(^1\Sigma_g^+)$ the solutions were prepared and filled into sample cells in a glovebox under a dry atmosphere to avoid uptake of humidity. These particular precautions were not necessary in the investigation of $O_2(^1\Delta_g)$.

The principal setup for the time-resolved measurements of the b → X, b → a, and a → X emissions of O_2 has been described.[17,21−23] Some changes have been made. We used as excitation source either an excimer laser (EMG 200) pumped dye laser (FL 3002) from Lambda Physik (380, 410 nm) or a Nd:YAG laser (Brilliant) from Quantel with frequency doubling or tripling (532, 355 nm). The sample housing was modified and allows now the simultaneous observation of up to three emissions. In this way, for example, the formation and decay of $O_2(^1\Sigma_g^+)$ and the rise of $O_2(^1\Delta_g)$, its successor in the deactivation cascade, can be followed simultaneously by their corresponding phosphorescence traces at 765, 1926, and 1276 nm. Three different detectors have been used: (1) a photomultiplier (PM R1464 Hamamatsu) with interference filter (IF 764 nm, half bandwidth, hbw = 19 nm) for time-resolved measurement of $O_2(^1\Sigma_g^+)$, (2) a liquid N_2-cooled InAs diode J12-D with preamplifier PA7 (EG&G Judson) equipped either with IF 1940 nm (hbw = 70 nm, transmissions at 1275 and 1588 nm ≤ 0.002) for the integral detection of $O_2(^1\Sigma_g^+)$ or with IF 1279 (hbw = 52 nm, transmission at 1926 nm ≤ 0.002) for the integral detection of $O_2(^1\Delta_g)$, (3) a fast liquid-N_2 cooled germanium diode (North Coast EO 817P) with IF 1275 (hbw = 40 nm) for time-resolved monitoring of $O_2(^1\Delta_g)$. The very fast decaying background fluorescence of the samples at 765 nm was separated from the extremely weak but slowly decaying b → X phosphorescence by means of a difference technique.[22,23] The emission experiments were averaged when necessary. With exception of H_2O we always used air-saturated solutions. The experiments have been performed at room temperature by varying the laser pulse energy. Only energy independent results are reported. Infrared absorption measurements have been done with a Perkin-Elmer Lambda 19 spectrophotometer.

Results

b → a Fluorescence. The quantum yield $Q_{b-a}(TET)$ of the b → a emission in CCl_4, which occurs at 1926 nm, has been determined in relative measurements using the a → X emission in C_6H_6 at 1277 nm as reference, as previously described in detail.[17] For the reference system we recently found $Q_{a-X}(BNZ) = (4.7 \pm 1.7) \times 10^{-5}$,[5] which corresponds to $k_{a-X}(BNZ) = 1.5 \pm 0.5\ s^{-1}$, if the $O_2(^1\Delta_g)$ lifetime of 31 μs in benzene is considered. Both emissions were isolated by filters IF 1940 or IF 1279. Hereby we took advantage that the InAs detector used behaves as a quantum counter in the respective wavelength range. Phenalenone (PHE), which sensitizes $O_2(^1\Sigma_g^+)$ with quantum yield $Q_\Sigma(TET) = 0.60$ [23] and $O_2(^1\Delta_g)$ with quantum yield $Q_\Delta(BNZ) = 0.98$ [24] was used in these measurements. Sample (PHE/TET) and reference (PHE/BNZ) solutions were optically matched at the excitation wavelength. $Q_{b-a}(TET)$ is obtained from the ratio of the excitation energy normalized and integrated signals I_{b-a} and I_{a-X} by eq 1, where $n(TET)$ and $n(BNZ)$ are the refractive indices and $T_{1940,\Sigma}$ and $T_{1279,\Delta}$ the filter transmissions for the b → a and a → X emissions, respectively.

$$Q_{b-a}(TET) = \frac{T_{1279,\Delta}\, n(TET)^2 Q_{a-X}(BNZ) Q_\Delta(BNZ) \int I_{b-a}(TET)\, dt}{T_{1940,\Sigma}\, n(BNZ)^2 Q_\Sigma(TET) \int I_{a-X}(BNZ)\, dt} \quad (1)$$

The lifetimes τ_Σ and τ_Δ of $O_2(^1\Sigma_g^+)$ and $O_2(^1\Delta_g)$ in sample and reference have additionally been determined by monitoring the respective time-resolved emissions with the PM and the fast Ge diode through the other emission ports. Quantum yields Q_{b-a} have been measured in the same way also in C_2Cl_4 and C_4Cl_6. It was assumed that the value $Q_\Sigma = 0.60$ determined for PHE in CCl_4 holds also true in these solvents. The main factor influencing the error limits of Q_{b-a} is the uncertainty of $Q_{a-X}(BNZ)$ of ± 33%.[5] IR absorption measurements showed that the solvents CCl_4, C_2Cl_4, and C_4Cl_6 neither absorb at 1930 nor at 1275 nm.

a → X Phosphorescence. With respect to Minaev's theory, the knowledge of both values k_{b-a} and k_{a-X} is of interest for a given solvent SOL. We therefore also monitored the rise curves of the a → X phosphorescence of sample PHE/SOL and reference PHE/BNZ in dependence of the laser pulse energy. Absolute values $k_{a-X}(SOL)$ are obtained from the maximum phosphorescence intensities $I_{a-X,m}$ and $Q_\Delta(BNZ) = 0.98$[24] by eq 2. The error limits of $k_{a-X}(SOL)$ are determined by the uncertainty of $k_{a-X}(BNZ)$. Since the same standard is used in both experiments, its uncertainty cancels in the ratios k_{a-X}/k_{b-a}, which have a smaller error limit of about ±20%.

$$k_{a-X}(SOL) = \frac{n(SOL)^2 I_{a-X,m}(SOL) Q_\Delta(BNZ) k_{a-X}(BNZ)}{n(BNZ)^2 I_{a-X,m}(BNZ) Q_\Delta(SOL)} \quad (2)$$

In addition to the k_{a-X}/k_{b-a} measurements, we determined values of k_{a-X} in several other solvents and in the binary solvent mixtures H_2O/acetone, acetone/C_6H_6, and $CH_3OH/CHCl_3$. Some precautions were necessary in these experiments. The solubility of O_2 is only small in H_2O. Therefore, in air-saturated H_2O the time constant of the rise of $O_2(^1\Delta_g)$ is only by about 1 order of magnitude smaller than the $O_2(^1\Delta_g)$ lifetime τ_Δ. Then, $I_{a-X,m}$ is no longer proportional to the initial concentration of $O_2(^1\Delta_g)$. In this case, we substituted $I_{a-X,m}(SOL)$ in eq 2 by the value of the entire integrated a → X emission intensity divided by τ_Δ. Of course, we also measured oxygenated solutions to shorten the rise time in H_2O. Both procedures gave the same results, indicating complete quenching of the triplet state of PHE by O_2 in air-saturated H_2O. The consideration of the solvent absorption in the range of the a → X emission wavelength is of importance for solvent molecules with O−H and O−D bonds, since these solvents exhibit significant vibrational overtone absorption. We measured at 1275 nm absorbances per centimeter of 0.475 (H_2O), 0.148 (CH_3OH), 0.082 (CF_3CH_2OH), and 0.068 (D_2O). Therefore, these solvents and mixtures with them act as an inner filter for the a → X emission. It was checked that the absorbance due to overtone absorption follows Lambert−Beer's law in solvent mixtures. The rest of investigated solvents do not significantly absorb in this wavelength range. To reduce the inner filter effect and the corresponding necessary correction, the defocused laser beam had to pass through a slit of 2 mm width, whose center was only 2 mm apart from the observation window of the cuvette. We took PHE as sensitizer in these measurements. PHE is a universal reference compound with a practically solvent independent value of Q_Δ. We recently determined for 13 different solvents of very different polarity and for mixtures H_2O/methanol $0.94 \le Q_\Delta \le 1.00$.[24] Therefore, we used for all the liquids with PHE the value $Q_\Delta = 0.98$ of

TABLE 1: Solvent Effect on the b → a and a → X Radiative Transitions of O_2[g]

solvent	Q_{b-a},[d] 10^{-4}	τ_Σ,[e] ns	k_{b-a},[d] 10^3 s^{-1}	k_{a-X},[d] s^{-1}	k_{a-X}/k_{b-a},[f] 10^{-4}	k^c_{b-a},[d] M^{-1} s^{-1}	k^c_{a-X},[d] M^{-1} s^{-1}	IP, eV
CCl_4[a]	4.5	130	3.4	1.1	3.2	330	0.11	11.47
CCl_4[b]	3.3	150	2.2	1.2	5.6	210	0.12	11.47
C_2Cl_4[b]	6.3	200	3.1	1.9	6.0	320	0.18	9.32
C_4Cl_6[b,c]	2.2	90	2.4	1.8	7.8	380	0.29	9.2

[a] Reference 17, $\lambda_{exc} = 337$ nm. [b] This work, $\lambda_{exc} = 380$ nm. [c] This work, $\lambda_{exc} = 410$ nm. [d] ±33%. [e] ±10%. [f] ±20%. [g] Each result is the mean value of at least five series of laser pulse energy dependent experiments.

TABLE 2: Solvent Effect on the a → X Radiative Transition of O_2[e]

solvent	k_{a-X},[a] s^{-1}	n	k^c_{a-X}, M^{-1} s^{-1}	P_{a-X}	R, mL mol^{-1}	V_{vdW},[b] mL mol^{-1}
D_2O	0.206	1.3384	0.00375	1.37×10^{-14}	3.67	11.5
H_2O	0.209	1.3328	0.00378	1.34×10^{-14}	3.71	11.5
CH_3OH	0.390	1.3290	0.0159	5.36×10^{-14}	8.29	21.7
CS_2[c]	3.14	1.6270	0.189	4.41×10^{-13}	21.3	31.2
CF_3CH_2OH	0.331	1.2900	0.0241	8.53×10^{-14}	13.2	38.8
CH_3COCH_3	0.543	1.3585	0.0399	1.17×10^{-13}	16.2	39.0
$CHCl_3$	0.96	1.4480	0.0770	2.14×10^{-13}	21.5	41.8
C_6H_6	1.50	1.5010	0.133	3.09×10^{-13}	26.2	48.4
CCl_4	1.17	1.4595	0.113	2.95×10^{-13}	26.4	49.8
CH_2I_2[d]	4.08	1.7430	0.329	6.21×10^{-13}	32.6	50.9
C_2Cl_4	1.89	1.5056	0.193	4.53×10^{-13}	30.3	56.5
C_6H_5I[c]	2.61	1.6190	0.291	5.66×10^{-13}	39.1	65.0
C_4Cl_6	1.85	1.5550	0.290	5.39×10^{-13}	50.3	90.1

[a] Uncertainty ±5% relative to k_{a-X}(BNZ) = 1.50; uncertainty of absolute value is ±33%. [b] Reference 34; sensitizers. [c] C_{60}, in the rest of solvents PHE. [d] Reference 8. [e] Each result of k_{a-X} is the mean value of at least 5 series of laser pulse energy dependent experiments.

C_6H_6. Since the absorptions of iodobenzene and CS_2 extend beyond 410 nm into the visible range, we took C_{60} with 532 nm excitation as sensitizer for these solvents, assuming that the value $Q_\Delta = 1$ determined in benzene and toluene[25] is also valid for other solvents.[8]

Tables 1 and 2 summarize our results for the pure liquids. The rate constants k_{a-X} determined in this study should be much more certain than our previously published values, since we (1) employed with PHE a sensitizer with a solvent independent quantum yield Q_Δ, (2) used only the superior time-resolved techniques, and (3) had better laser systems. Considering the experimental uncertainties of our earlier published k_{a-X} data,[7] we observe for D_2O (old: 0.30 s^{-1}) and CS_2 (old: 1.0 s^{-1}, steady-state luminescence measurement without sufficient control of τ_Δ) large changes. Inspection of the k_{a-X} compilation reveals a significant difference only for CF_3CH_2OH (0.17 s^{-1}).[8] The reason for this large deviation is not known.

Discussion

Intensity Borrowing. According to Minaev, collisions induce different dipole moments M_x and M_y in the MOs $\pi_{g,x}$ and $\pi_{g,y}$ of O_2 as a result of an admixture of the collider's MOs. Hereby, electric dipole character is induced into the b → a transition. Quantitatively, the transition moment of the collision-induced b → a transition should be determined by the difference of the induced dipole moments: $\mathbf{M}_{b-a} = 0.5(M_x - M_y)$.[19] Since the spin−orbit coupling (SOC) of oxygen is strong, the $X^3\Sigma_g^-$ ground state of O_2 has some $b^1\Sigma_g^+$ character. The admixture coefficient is given by $C = \zeta/E_\Sigma$, where $\zeta = 176$ cm^{-1} and $E_\Sigma = 13\,121$ cm^{-1} are the SOC constant of O_2 and the $b^1\Sigma_g^+$ excitation energy, respectively.[2,19,26] Because of the mixing of the $b^1\Sigma_g^+$ and $X^3\Sigma_g^-$ states, the a → X transition can profit from the collision-induced enhancement of the b → a transition by intensity borrowing. Minaev obtained for the corresponding transition moment $\mathbf{M}_{a-X} = -C\mathbf{M}_{b-a}$, leading with $E_\Delta = 7882$ cm^{-1} to eq 3. Thus, in the simple form of the theory the ratio k_{a-X}/k_{b-a} should in principle be determined by the SOC constant of O_2.

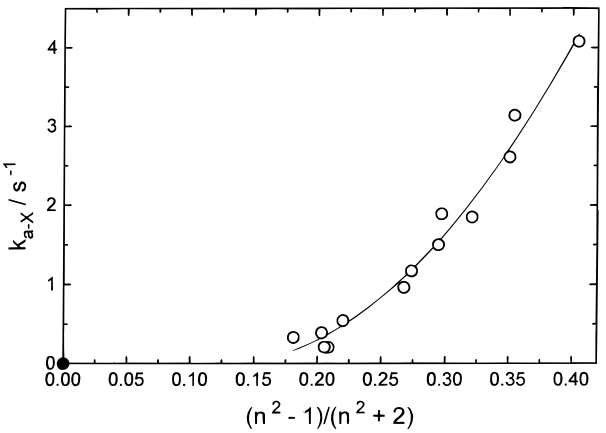

Figure 1. Correlation of k_{a-X} with the bulk polarizability P of pure solvents: (curve) polynomial fit ($k_{a-X} = 0.798 - 13.08P + 52.96P^2$ s^{-1}) to the data of Table 2 (open circles); (solid circle) k_{a-X} in the diluted gas.

$$\frac{k_{a-X}}{k_{b-a}} = \frac{C^2 {E_\Delta}^3}{(E_\Sigma - E_\Delta)^3} \qquad (3)$$

With the theoretically derived coefficient $C = 0.0134$ the ratio k_{a-X}/k_{b-a} is calculated to be 6.1×10^{-4}.[19] We obtain experimentally moderately varying ratios k_{a-X}/k_{b-a}; see Table 1. The average ratio for the three solvents investigated is 6×10^{-4}. The phonon-induced radiative transitions a → X and b → a dominate at 5 K in solid Ar, where Becker et al. determined $k_{a-X} = 1.27 \times 10^{-2}$ s^{-1} and $k_{b-a} = 41$ s^{-1}.[27] From these data $k_{a-X}/k_{b-a} = 3.1 \times 10^{-4}$ results. Although we find not the constant ratio expected from eq 3, it is still surprising how good the simple theory predicts the magnitude of the ratio k_{a-X}/k_{b-a}. These results confirm Minaev's basic idea that the rate constant of the a → X transition borrows intensity from the collision-induced radiative processes b → a via SOC.

Minaev showed in a more refined treatment that charge-transfer interactions between the collider and O_2 should lead to an additional but minor enhancement of the a → X radiative transition.[19] Therefore, an increase of k_{a-X}/k_{b-a} with decreasing ionization potential (IP) of the collider could be expected. A closer inspection demonstrates that the values k_{a-X} and the ratios k_{a-X}/k_{b-a} increase with decreasing IP in the series CCl_4 to C_4Cl_6. Thus, an additional source of intensity enhancement of the a → X transition could actually be operating.

Solvent Dependence of the Rate Constant k_{a-X}. We measured rate constants k_{a-x} in several pure liquids of varying bulk polarizability P and in the binary solvent mixtures H_2O/acetone, acetone/C_6H_6, and $CH_3OH/CHCl_3$. In Figure 1 we plot first-order rate constants k_{a-X} determined in pure liquids vs P. A rather smooth and slightly upward curved correlation is obtained, very similar to those shown in ref 8. However, no continuous smooth fit of functions of P to the data is possible, if we also include the gas-phase value $k_{a-X} = 2.6 \times 10^{-4}$ s^{-1} at $P = 0$;[3] see the solid circle in Figure 1.

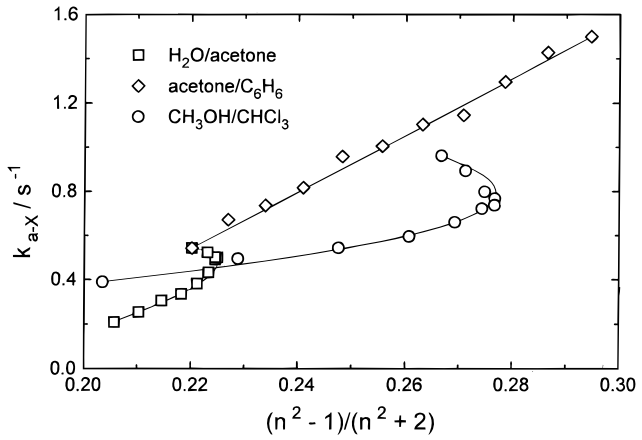

Figure 2. Correlation of k_{a-X} with the bulk polarizability of solvent mixtures; experimental error of the k_{a-X} data ±5%. The graduation in the mixture composition is always 10 wt %; the connecting lines are calculated according to eqs 4 to 6. For details, see text.

Actually, no general form of correlation of k_{a-X} with P exists, even if we consider only solution phase data, as is demonstrated by the corresponding plot of k_{a-X} vs P for the solvent mixtures shown in Figure 2. In contrast to the slightly upward curved correlation for the pure liquids of Figure 1, we see in Figure 2 different forms of correlations of k_{a-X} with P: a linear variation of k_{a-X} for acetone/C_6H_6, and two strongly bent anomalous curves for H_2O/acetone and $CH_3OH/CHCl_3$, both even passing through a maximum of P. A similar anomalous dependence of k_{a-X} on P was already recently found by Bilski et al. for D_2O/acetonitrile.[16] Thus, correlations such as the one of Figure 1 do not reveal the actual physical processes causing the solvent effect on k_{a-X}.

Bilski et al. reported that the value of k_{a-X} in H_2O should only be about half the value in D_2O.[16] This result is wrong. It was neglected that H_2O and to a minor extent also D_2O absorb in the wavelength range of the a → X emission, vide supra. In fact, we determine for H_2O and D_2O the same values of k_{a-X}, if we correct for this inner filter. The very steep dependence of k_{a-X} on P presented by Bilski et al. for D_2O/acetonitrile, passing also through a maximum of P, is only slightly perturbed by the neglect of the weak inner filter of D_2O. This anomalous variation of k_{a-X} with P was interpreted by the assumption of specific interactions between $O_2(^1\Delta_g)$ and acetonitrile. It was speculated that complex formation between $O_2(^1\Delta_g)$ and the π bonds of the −CN moiety could be the reason for the very strong increase of k_{a-X} with the concentration of acetonitrile in the mixture.[16]

However, this actually is not the case. Having realized that the collision-induced a → X emission is a bimolecular process, it can very easily be shown that the anomalous dependence of k_{a-X} on P in solvent mixtures is not the consequence of some specific interactions between $O_2(^1\Delta_g)$ and a mixture component but instead only caused by specific interactions between the components of the mixture. Second-order rate constants k^c_{a-X} of the collision-induced a → X radiative transition have been calculated from pseudo-first-order rate constants k_{a-X} using the molarity of the pure liquids. These data are listed in Table 2.

Collisions of $O_2(^1\Delta_g)$ with molecules A and molecules B contribute independently to the overall probability of the radiative transition in mixtures of solvents A and B. Each contribution is given by the product of the second-order rate constant and the corresponding concentration. Thus, eq 4 holds true for k_{a-X}. Equation 5 gives the molar concentration of component A in the mixture, where x_A and ΔV_{exc} are the molar fraction of A and the concentration dependent excess volume

$$k_{a-X} = k^c_{a-X,A}[A] + k^c_{a-X,B}[B] \quad (4)$$

$$[A] = \frac{x_A}{x_A(V_{m,A} - V_{m,B}) + V_{m,B} + \Delta V_{exc}} \quad (5)$$

of the mixture, respectively. Finally, the bulk polarizability of a mixture is calculated with rather high certainty by eq 6 from the molar refractions $R = V_m(n^2 - 1)/(n^2 + 2)$, with V_m being the molar volume.[28]

$$P = R_A[A] + R_B[B] \quad (6)$$

The accuracy of the calculated data of P is high, even for mixtures with anomalous dependence of P on the component concentration. This is exemplarily verified for the mixture of acetone and H_2O, for which the refractive index n[29] as well as the density ρ[30] have precisely been determined as a function of the mixture composition. Table 3 compares values of P based on the experimental data of n with bulk polarizabilities P_{calc} calculated by eqs 5 and 6 with the values of ΔV_{exc}, whereby the latter are derived from the concentration dependent density data. The experimental maximum of P in the concentration dependence is actually reproduced by the calculation. The maximum deviation of P_{calc} from P amounts to only 0.0009 or 0.4%. Using the older data of n and ρ determined by Drude at 16 °C for the mixtures H_2O/acetone and acetone/C_6H_6 results also in only small deviations of P_{calc} from P. These amount at maximum to 0.4% (H_2O/acetone) and −0.4% (acetone/C_6H_6).[31] These findings demonstrate that the calculation of the bulk polarizability leads to reliable results, if it is based on the molar refractions of the components and on ΔV_{exc} data. We therefore calculated the values of P for the mixtures by eqs 5 and 6 and the ΔV_{exc} data resulting from literature.[30,32,33]

The different forms of correlations of k_{a-X} with P in Figure 2 are simply caused by the different molecular interactions between the components of the three mixtures. The anomalous dependences of k_{a-X} on P in H_2O/acetone and $CH_3OH/CHCl_3$ are the consequences of strongly attractive interactions, which lead to distinctly negative excess volumes ΔV_{exc}. For H_2O/acetone the maximum value of ΔV_{exc} amounts at 25 °C to −1.6 mL (70 wt % acetone) (see Table 3), which is significant compared with the molar volumes 73.5 mL mol^{-1} (acetone) and 18.0 mL mol^{-1} (H_2O).[30] For $CH_3OH/CHCl_3$ the solvent contraction at 25 °C is even larger with the maximum value of ΔV_{exc}= −8.6 mL (59 wt % CH_3OH), compared with V_m = 40.7 mL mol^{-1} (CH_3OH) and V_m = 80.7 mL mol^{-1} ($CHCl_3$).[32] In contrast, the mixture acetone/C_6H_6 behaves at 20 °C almost ideally with the maximum value of ΔV_{exc}= −0.07 mL (40 wt % acetone).[33]

The two curves and the straight line connecting the k_{a-X} data of the pure mixture components, which are drawn in Figure 2, match the experimental rate constants k_{a-X} of the mixtures quite well. It should be noted that they are not results of fits but simply calculated using eqs 4−6 and the values of k^c_{a-X} and R, given in Table 2, taking into account the literature data of ΔV_{exc}.[30,32,33] Thus, anomalous as well as almost ideal behavior is reproduced without inferring specific interactions of $O_2(^1\Delta_g)$ with some component of the mixture. The interactions of $O_2(^1\Delta_g)$ with the colliders, which induce the a → X radiative transition, are already included in the corresponding bimolecular rate constant k^c_{a-X}. The results of the solvent mixtures definitely demonstrate the bimolecularity of the emission process also in the liquid phase. We conclude that eq 4 can also be used to calculate values of k_{a-X} in compressed gases and gas mixtures.

TABLE 3: Comparison of Experimental and Calculated Bulk Polarizabilities of Mixtures of Acetone (ACT) and H_2O at 25 °C[a]

ACT wt %	x_{ACT}	n[a]	P	ρ,[b] g mL^{-1}	ΔV_{exc}, mL	[ACT], M	[H_2O], M	P_{calc}
0	0	1.3326	0.2055	0.9971	0.000	0.000	55.331	0.2055
10	0.0333	1.3401	0.2097	0.9831	−0.248	1.693	49.098	0.2097
20	0.0720	1.3470	0.2135	0.9696	−0.538	3.339	43.043	0.2138
30	0.1174	1.3529	0.2168	0.9549	−0.840	4.932	37.092	0.2175
40	0.1714	1.3579	0.2195	0.9371	−1.101	6.454	31.202	0.2203
50	0.2368	1.3609	0.2212	0.9169	−1.316	7.893	25.440	0.2221
60	0.3176	1.3635	0.2226	0.8946	−1.470	9.242	19.858	0.2232
70	0.4199	1.3645	0.2232	0.8711	−1.559	10.499	14.502	0.2237
80	0.5538	1.3638	0.2228	0.8450	−1.460	11.638	9.378	0.2231
90	0.7363	1.3616	0.2216	0.8165	−1.053	12.652	4.531	0.2215
100	1	1.3570	0.2190	0.7849	0.000	13.514	0.000	0.2186

[a] Experimental refractive indices n at 25 °C;[29] values of P calculated from n. [b] Densities ρ at 25 °C are interpolated values of density data measured at 20 °C and 40 °C;[30] excess volumes ΔV_{exc} calculated from ρ at 25 °C; concentrations [ACT], [H_2O], and bulk polarizabilities P_{calc} calculated by eqs 5 and 6 on the basis of the data of ΔV_{exc}.

A closer examination shows that for the mixtures H_2O/acetone and $CH_3OH/CHCl_3$ only the bulk polarizability P passes through a maximum value with increasing concentrations of acetone or $CHCl_3$ but not the rate constant k_{a-X}, although eqs 4 and 6 have the same formal concentration dependence. The reason for that different reaction on the volume contraction of the mixtures lies in the very different magnitude of variation of k_{a-X} and P. Because of the large increase of k_{a-X} (by 160% and 145%, respectively), the volume contraction of the mixture can only cause a moderate deviation from linearity in the concentration dependence of k_{a-X}. In contrast, P increases only very little (by 7% and 31%, respectively). Therefore, the concentration dependence of P deviates strongly from linearity, leading even to maximum values.

Mechanism of the Solvent Perturbation of the a → X Radiative Transition. The solvent dependence of the second-order rate constants k^c_{a-X} is strong. The data of Table 2 vary by a factor of about 100 from 0.0038 (D_2O) to 0.33 M^{-1} s^{-1} (CH_2I_2). The question arises, which parameters determine this large variation of k^c_{a-X}? The strong enhancement of the b → a fluorescence is a consequence of the electric dipole character of the b → a transition in collisions, caused by the admixture of the colliding molecule's orbitals to the $\pi_{g,x}$ and $\pi_{g,y}$ MOs of O_2.[19] Starting from this fundamental concept of Minaev, we showed that this asymmetrical transient charge shift depends on the molecular polarizability of the colliding molecule, which is expressed in the range of optical frequencies by the molar refraction R. By the analysis of two different data sets we recently found k^c_{a-X} proportional to R^s. Using only our own data,[6] we determined the exponent s to be 1.71 ± 0.08. With the data of k^c_{a-X} calculated from the compilation of Ogilby et al.[8] we obtained $s = 1.93 \pm 0.10$.[17] Since the fitted exponents of R were only a little smaller than 2, we concluded that for a hypothetical set of colliders of the same shape, size, and mass but of different molecular polarizability, for which collision distance and collision frequency would be constant, a pure quadratic dependence on R should exist. Then, the collision-induced transition moment would directly be proportional to the molar refraction R.

Figure 3 plots the data of k^c_{a-X} of Table 2 in a double-logarithmic plot vs R. A linear least-squares fit through all the data results in a straight line with slope $s = 1.84 \pm 0.12$ (not shown). Thus, a general strong correlation of $\log(k^c_{a-X})$ with $\log(R)$ exists, in agreement with our previous investigation. However, a closer look on the data reveals significant gradu-

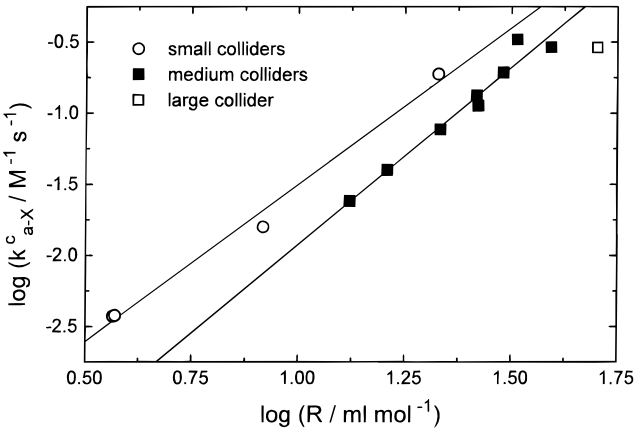

Figure 3. Double-logarithmic plot of k^c_{a-X} vs the molar refraction R of collider; data of Table 2. The straight lines represent linear least-squares fits to the data of the small (1) and medium size (2) colliders: (1) slope 2.21 ± 0.15; (2) slope 2.49 ± 0.20. For details, see text.

ations. If only the data of the medium size colliders with van der Waals volumes $38.8 \leq V_{vdW} \leq 65.0$ mL mol^{-1} are considered[34] (see Table 2), our fit yields $s = 2.49 \pm 0.20$. The resulting straight line is drawn in Figure 3. The data for the four small colliders H_2O, D_2O, CH_3OH, and CS_2, with $V_{vdW} \leq 31.2$ mL mol^{-1} lie all distinctly above this straight line but still correlate similarly strong with $\log(R)$, as is demonstrated by the corresponding fitted straight line with slope $s = 2.21 \pm 0.15$. In contrast, the value for the large collider C_4Cl_6 ($V_{vdW} = 90.1$ mL mol^{-1}) lies distinctly below. Obviously, there are also other factors besides the molecular polarizability influencing the values of k^c_{a-X}. A possible effect of the collider polarity on k^c_{a-X}, however, is completely hidden behind the dominating effect of R.

(1) We have to keep in mind that the investigations were done in liquids of strongly varying refractive index: $1.290 \leq n \leq 1.743$. The effect of the refractive index of the surrounding medium on the radiative rate constant was experimentally investigated by the comparison of the absorption spectra of 9-methylanthracene in the vapor phase and in cyclohexane.[35] The results strongly support the proportionality of the radiative rate constant with n^2.

(2) We deal with real molecular colliders of different size, shape, and mass, which leads to different collision frequencies. Furthermore, the colliders are composed of atoms with in part very different atomic polarizability (atomic refraction). Therefore, the mobility of electron density varies not only with the collider but also with the atomic position on the collider molecule. We see no possibility to consider such variations in a general analysis of k^c_{a-X} data. However, we can account for variations of the normalized collision frequency Z by eq 7 , if

$$Z = d_{OC}{}^2 N_A \sqrt{8\pi kT/\mu} \qquad (7)$$

we approximate the colliders and O_2 as spheres. In eq 7 $d_{OC} = (d_{O_2} + d_C)/2$ and μ are the collision distance and the reduced mass of the colliding pair, which can be calculated from $d_{O_2} = 3.45$ Å, $d_C = (6V_{vdW}/\pi N_A)^{1/3}$ and the respective molecular weights. N_A is Avogadro's number, k the Boltzmann constant, and T the Kelvin temperature. The collision frequency in the liquid phase is by the value of the pair distribution function at a contact distance larger than the gas-phase value Z.[36] Assuming the model of hard sphere liquids, such values could be estimated, if the compressibilities of the liquids were known.[37,38] However, since for several of the investigated solvents compressibility

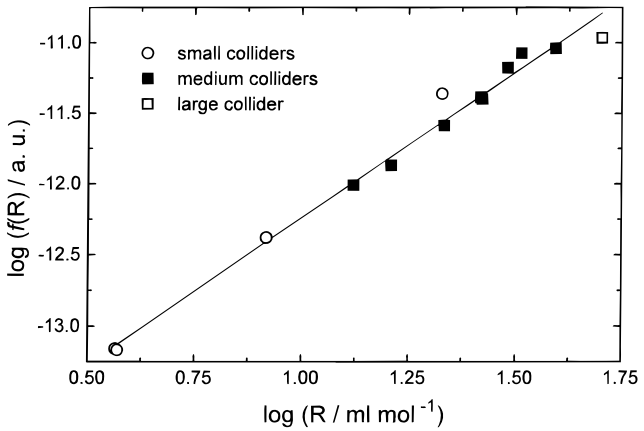

Figure 4. Double-logarithmic plot of $f(R)$ vs the molar refraction R of collider. Straight line represents linear least-squares fit with slope 2.06 ± 0.08 and intercept -14.30 ± 0.09. For details, see text.

data are lacking, we only can calculate the normalized gas-phase collision frequency, which varies from 1.5×10^{11} (D_2O) to 2.2×10^{11} (C_4Cl_6) M^{-1} s^{-1}. Using these numbers, extremely low probabilities $P_{a-X} = k^c_{a-X}/(Zn^2)$ of the collision-induced radiative transition per collision, which are normalized to $n = 1$, are obtained, ranging from 1.4×10^{-14} (H_2O) to 5.7×10^{-13} (C_4Cl_6).

(3) The effect of collider size on $\log(k^c_{a-X})$, illustrated in Figure 3, can be understood if the mechanism of the collision-induced radiative transition is considered. Only those MOs of the colliding molecule, which overlap with the $\pi_{g,x}$ and $\pi_{g,y}$ MOs of O_2 in the collision, strongly contribute to the enhancement of the a $\rightarrow$ X radiative transition by a transient shift of electron density. Those MOs, which are farther away from O_2 in the collision complex, of course, contribute less or nothing. If we compare a small and a large collider of the same value of R, the molecular polarizability has therefore a smaller effect in the case of the large collider. This is the principal reason, in Figure 3, why the data of $\log(k^c_{a-X})$ of the small colliders all lie above the straight line, fitted to the medium size colliders, and the log-
(k^c_{a-X}) value of the large collider lies below. Therefore, the probability P_{a-X} of the collision-induced radiative transition per collision depends not only on the molecular polarizability but also on the size (actually the molecular structure) of the collider. If we consider in our generalizing analysis the colliders simply as spheres of uniform polarizability, the transition probability still depends at least on R and V_{vdW}. We approximate $P_{a-X} = f(R)g(V_{vdW})$ as a product of two functions, whereby the functions $f(R)$ and $g(V_{vdW})$ separately describe the dependences of P_{a-X} on the molecular polarizability and on the size of the collider, respectively. Different empirical functions $g(V_{vdW})$ could be assumed. Only those are expected to be realistic, for which the correlation of $f(R) = P_{a-X}/g(V_{vdW})$ vs R becomes independent of the collider size. Figure 4 plots $f(R)$ in a double-logarithmic plot vs R. A smooth linear correlation results. The linear least-squares fit of all the data now also describes the data for the small colliders H_2O, D_2O, and CH_3OH reasonably well; compare Figure 3. Only two values, one for a large (C_4Cl_6) and one for a small (CS_2) collider, still moderatly deviate from the straight line. Thus, the empirical function $g(V_{vdW}) = V_{vdW}{}^{-2/3}$, which has been used in the calculation of the $f(R)$ data of Figure 4, reasonably accounts for the size dependence of P_{a-X}.

The physical meaning of the size correction function $g(V_{vdW})$ can be understood, if the colliders are considered as spheres of uniform polarizability. Then, the overall-surface of the collider is proportional to $V_{vdW}{}^{2/3}$. The transient shift of electron density into the $\pi_{g,x}$ and $\pi_{g,y}$ MOs of O_2 can only take place in the small contact region of O_2 and collider, where the MOs mutual overlap. As long as the area of the contact region is constant in the series of colliders, its relative magnitude varies with the collider size approximately proportional to $V_{vdW}{}^{-2/3}$. Therefore, $g(V_{vdW}) = V_{vdW}{}^{-2/3}$ is proportional to that part of the collider polarizability, which becomes effective in the collision-induced a $\rightarrow$ X radiative transition.

The linearity of the correlation of $\log(f(R))$ with $\log(R)$ shows that a correlation of $f(R)$ with R with zero or only a negligible intercept exists. The slope of the linear least-squares fit of Figure 4 amounts to $s = 2.06 \pm 0.08$. Thus, the analysis of the double-logarithmic plot reveals that $f(R) \sim R^2$. After having removed the size dependence of P_{a-X}, we realize that the probability of the collision-induced a $\rightarrow$ X emission is directly proportional to the square of the molecular polarizability of the collider. Since radiative rate constants are proportional to the square of the transition moment $\mathbf{M}$, we finally find the direct and linear proportionality $\mathbf{M_{a-X}} \sim R$ for the bimolecular radiative transition as the principal reason for the solvent effect on k_{a-X}. Of course, also other but minor important sources of intensity enhancement may contribute, vide supra.

This result is surprisingly simple but seems rather reasonable. Minaev derived $\mathbf{M_{b-a}} = 0.5(M_x - M_y)$ and $\mathbf{M_{a-X}} = -C\mathbf{M_{b-a}}$, whereby M_x and M_y are the dipole moments induced into the $\pi_{g,x}$ and $\pi_{g,y}$ MOs of O_2 during the collision.[19] Therefore, the transition moment of the a $\rightarrow$ X transition depends indirectly but also linearly on that difference: $\mathbf{M_{a-X}} \sim (M_x - M_y)$. Our experimental result $\mathbf{M_{a-X}} \sim R$ demonstrates that the difference of the induced dipole moments linearly depends on the *molecular polarzability of the collider*. Obviously, a transient shift of electron density from MOs of the collider to the only partially filled $\pi_{g,x}$ and $\pi_{g,y}$ MOs of O_2 occurs.

Dipole moments can be induced not only by this pure dispersion interaction but, of course, also by induction interaction of permanent collider dipole moments with the nonpolar O_2 molecule. This induction interaction, which depends on the *molecular polarizability of O_2*, also leads to a different polarization of the $\pi_{g,x}$ and $\pi_{g,y}$ MOs and should therefore also contribute to the enhancement of the radiative transitions. However, since any polarity effect disappears behind the strong dependence of k^c_{a-X} on the molecular polarizability of the collider, the pure dispersion interaction must be much stronger than the induction interaction. Actually, calculations performed for simple molecules show that dispersion interactions are much stronger than induction interactions.[39]

Conclusions

Although we have not performed theoretical calculations, our generalizing analysis of the experimental data revealed the principal mechanism of the solvent perturbation of the a $\rightarrow$ X radiative transition. According to Minaev, two effects cooperate in the collision-induced emission process. (1) The asymmetric shift of electron density from the collider into the $\pi_{g,x}$ and $\pi_{g,y}$ molecular orbitals of O_2 induces electric dipole character into the b $\rightarrow$ a transition. (2) Because of the strong SOC of O_2, the a $\rightarrow$ X transition profits directly from the enhancement of the b $\rightarrow$ a transition by intensity borrowing. This theoretically derived result is confirmed by our experiments. We have shown that the perturbed radiative transition is clearly a bimolecular process, also in the liquid phase. For mixtures, k_{a-X} is additively composed of the contributions of the individual components. Hereby, each contribution is given by the product of concentra-

tion and corresponding second-order rate constant k^c_{a-X}. For pure solvents, k^c_{a-X} correlates roughly with the square of the molar refraction R of the solvent. Hereby a graduation according to the molecular size of the collider is observed. If the effects of the solvent refractive index, of the collision frequency, and of the dependence of the probability of the radiative transition on the size of the collider are removed, it is discovered that the indirectly induced dipole strength of the a $\rightarrow$ X radiative transition increases with the square of the molecular polarizability of the collider. These findings explain for the first time consistently and quantitatively the solvent effect on k_{a-X}.

Since the a $\rightarrow$ X and b $\rightarrow$ a emissions are closely connected by SOC, we expect that the directly induced dipole strength of the b $\rightarrow$ a radiative transition also mainly depends on R^2 in solution. Actually, this assumption gets support from the analysis of the gas-phase data of k^c_{b-a} of Fink et al.,[40] which we previously performed.[17] Experiments on the solvent effect on k^c_{b-a}, including solvents in which the lifetime of $O_2(^1\Sigma_g^+)$ is too short for emission experiments, have now become possible by means of measurements of the transient a $\rightarrow$ b absorption of $O_2(^1\Delta_g)$ in solution.[41,42] These experiments will show whether such expectations are justified.

Acknowledgment. Financial support by the Deutsche Forschungsgemeinschaft and the Fonds der Chemischen Industrie is gratefully acknowledged.

References and Notes

(1) Herzberg, G. *Spectra of Diatomic Molecules*; Van Nostrand Reinhold: New York, 1950; p 560.
(2) Klotz, R.; Marian, C. M.; Peyerimhoff, S. D.; Hess, B. A.; Buenker, A. J. *Chem. Phys.* **1984**, *89*, 223.
(3) Badger, R. M.; Wright, A. C.; Whitlock, R. F. *J. Chem. Phys.* **1965**, *43*, 4345.
(4) Scurlock, R. D.; Ogilby, P. R. *J. Phys. Chem.* **1987**, *91*, 4599.
(5) Schmidt, R. *Chem. Phys. Lett.* **1988**, *151*, 369.
(6) Schmidt, R.; Afshari, E. *J. Phys. Chem.* **1990**, *94*, 4377.
(7) Losev, A. P.; Nichiporovich, I. N.; Byteva, I. M.; Drozdov, N. N.; Al Jghgami, I. F. *Chem. Phys. Lett.* **1991**, *181*, 45.
(8) Scurlock, R. D.; Nonell, S.; Braslavsky, S. E.; Ogilby, P. R. *J. Phys. Chem.* **1995**, *99*, 3521.
(9) Darmanyan, A. P. *Chem. Phys. Lett.* **1993**, *215*, 477.
(10) Losev, A. P.; Byteva, I. M.; Gurinovich, G. P. *Chem. Phys. Lett.* **1988**, *143*, 127.
(11) Gorman, A. A.; Hamblett, I.; Lambert, C.; Prescott, A. L.; Rodgers, M. A. J.; Spence, H. M. *J. Am. Chem. Soc.* **1987**, *109*, 3091.
(12) Gorman, A. A.; Krasnovsky, A. A.; Rodgers, M. A. J. *J. Phys. Chem.* **1991**, *95*, 598.
(13) Darmanyan, A. P.; Foote, C. S. *J. Phys. Chem.* **1993**, *97*, 5032.
(14) Darmanyan, A. P.; Foote, C. S. *J. Phys. Chem.* **1992**, *96*, 6317.
(15) Krasnovsky, A. A.; Yegorov, S. Y.; Nazarova, O. V.; Yartsev, Y. I.; Ponomarev, G. V. *Biofysica* **1987**, *32*, 982.
(16) Bilski, P.; Holt, R. N.; Chignell, C. F. *J. Photochem. Photobiol. A: Chem.* **1997**, *109*, 243.
(17) Schmidt, R.; Bodesheim, M. *J. Phys. Chem.* **1995**, *99*, 15919.
(18) Minaev, B. F. *J. Prikl. Spectrosk.* **1985**, *42*, 766.
(19) Minaev, B. F.; Lunell, S.; Kobzev, G. I. *J. Mol. Struct. (THEOCHEM)* **1993**, *284*, 1.
(20) Noxon, J. F. *Can. J. Phys.* **1961**, *39*, 1110.
(21) Schmidt, R.; Bodesheim, M. *J. Phys. Chem.* **1994**, *98*, 2874.
(22) Schmidt, R.; Bodesheim, M. *Chem. Phys. Lett.* **1993**, *213*, 111.
(23) Bodesheim, M.; Schütz, M.; Schmidt, R. *Chem. Phys. Lett.* **1994**, *221*, 7.
(24) Schmidt, R.; Tanielian, C.; Dunsbach, R.; Wolff, C. *J. Photochem. Photobiol. A: Chem.* **1994**, *79*, 11.
(25) Terazima, M.; Hirota, N.; Shinohara, H.; Saito, Y. *J. Phys. Chem.* **1991**, *95*, 9080.
(26) Minaev, B. F.; Agren, H. *J. Chem. Soc., Faraday Trans.* **1997**, *93*, 2231.
(27) Becker, A. C.; Schurath, U.; Dubost, H.; Galaup, J. P. *Chem. Phys.* **1988**, *125*, 321.
(28) Tomlinson, W. J.; Chandross, E. A. *Adv. Photochem.* **1980**, *12*, 201.
(29) Ernst, R. C.; Litkenhous, E. E.; Spanyer, J. W. *J. Phys. Chem.* **1932**, *36*, 842.
(30) Hellwege, K.-H., Ed. *Landolt-Börnstein, Neue Serie, Band 1, Dichten flüssiger Systeme, Teil b*; Springer-Verlag: Berlin, 1977; p 134.
(31) Drude, P. *Z. Phys. Chem.* **1897**, *23*, 267.
(32) Hellwege, K.-H., Ed. *Landolt-Börnstein, Neue Serie, Band 1, Dichten flüssiger Systeme, Teil a*; Springer-Verlag: Berlin, 1974; p 208.
(33) Hellwege, K.-H., Ed. *Landolt-Börnstein, Neue Serie, Band 1, Dichten flüssiger Systeme, Teil a*; Springer-Verlag: Berlin, 1974; p 227.
(34) Bondi, A. *J. Phys. Chem.* **1964**, *68*, 441.
(35) Hirayama, S.; Phillips, D. *J. Photochem.* **1980**, *12*, 139.
(36) Einwohner, T.; Alder, B. *J. Chem Phys.* **1968**, *49*, 1548.
(37) Schmidt, R. *J. Phys. Chem. A* **1998**, *102*, 9082.
(38) Hild, M.; Brauer, H.-D. *Chem. Phys. Lett.* **1998**, *283*, 21.
(39) Kauzmann, W. *Quantum Chemistry*; Academic Press: New York, 1957; p 516.
(40) Fink, E. H.; Setzer, K. D.; Wildt, J.; Ramsay, D. A.; Vervloet, M. *Int. J. Quantum Chem.* **1991**, *39*, 287.
(41) Weldon, D.; Ogilby, P. R. *J. Am. Chem. Soc.*, **1998**, *120*, 12978.
(42) We have been informed in a recent private communication that A. P. Losev (Minsk) has also detected $O_2(^1\Delta_g)$ in solution-phase absorption.